Efficient Coupled Oxidation of Heme by an Active Site Variant of Horse Heart Myoglobin

Dean P. Hildebrand,[1a] Hai-lun Tang,[1a−c] Yaoguang Luo,[1a] Christie L. Hunter,[1a] Michael Smith,[1a,b] Gary D. Brayer,[1a] and A. Grant Mauk*,[1a]

Contribution from the Department of Biochemistry and Molecular Biology, Biotechnology Laboratory, and Protein Engineering Network of Centres of Excellence, University of British Columbia, Vancouver, British Columbia V6T 1Z3, Canada

Received June 14, 1996[⊗]

Abstract: The coupled oxidation of protoheme IX at the active sites of heme proteins exposed to ascorbate in the presence of dioxygen has been known for over 65 years and is related to the catalytic conversion of protoheme IX to biliverdin by the enzyme heme oxygenase. The present report demonstrates that replacement of two residues present in the distal heme pocket of horse heart myoglobin (Mb), Val67 and Val68, with alanine and serine, respectively, increases the efficiency of coupled oxidation in the active site of myoglobin. HPLC analysis of the heme oxidation product demonstrates that the specificity of wild-type myoglobin for opening the heme ring at the α-*meso* carbon is retained by the variant. The infrared spectrum of the carbonyl derivative of the variant exhibits ν_{CO} bands of comparable intensity at 1948 and 1958 cm^{-1}, which are consistent with the presence of the polar serine residue in close proximity to the bound ligand. The high-resolution crystal structure of the Val67Ala/Val68Ser metMb variant establishes that a hydrogen bond forms between the hydroxyl group of Ser68 and the coordinated water molecule. The increased rate of coupled oxidation exhibited by the variant is attributed to the increased polarity of the distal pocket created by the amino acid substitutions. These results are discussed in light of recent work concerning the active site of heme oxygenase.

Oxidation of protoheme IX to α-biliverdin is catalyzed metabolically by the hepatic membrane-bound enzyme heme oxygenase.[1,2] Although recent progress in the expression and characterization of a soluble fragment of heme oxygenase has resulted in considerable progress in our understanding of this enzyme,[3] many uncertainties concerning the catalytic mechanism of heme oxygenase persist. One obvious factor that hinders development of such a mechanism is the current lack of a three-dimensional structure for this enzyme. One means of gaining insight into possible mechanistic options that may be exercised by heme oxygenase is to consider the process referred to as coupled oxidation that occurs upon exposure of myoglobin and other heme-containing proteins to ascorbate.[4]

As is the case for the reaction catalyzed by heme oxygenase, coupled oxidation results in the oxidative cleavage of protoheme IX to produce Fe(III)-biliverdin through the intermediate formation of α-hydroxyheme and verdoheme (Figure 1).[5] The coupled oxidation of protoheme IX pyridine hemochromagen in the absence of protein results in a random mixture of the four possible Fe(III)-biliverdin isomers that result from oxidative cleavage at the four *meso* (α, *β*, *γ*, and *δ*) positions, whereas the reaction of heme bound at the active site of Mb results in cleavage at the α-*meso* position exclusively.[6] The isomer composition observed following coupled oxidation of various heme proteins has been shown to be correlated with the accessibility of the dioxygen bound to the heme iron toward

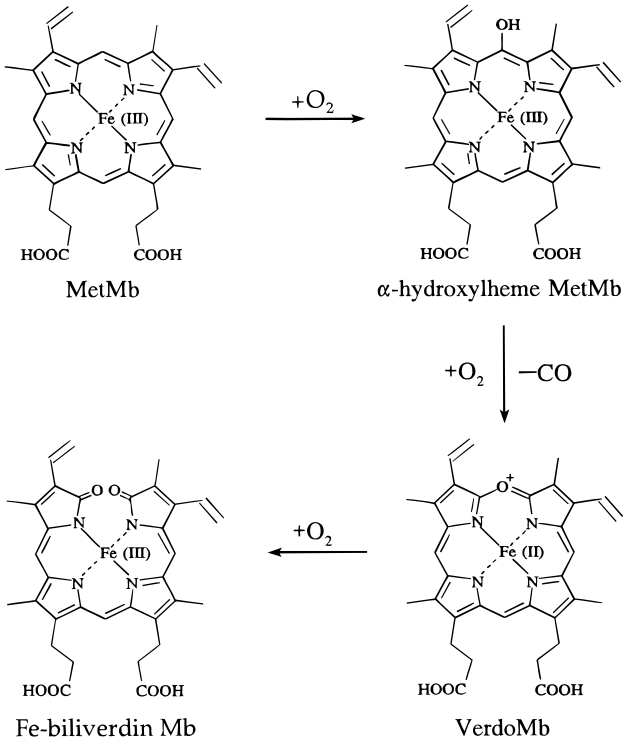

Figure 1. Proposed reaction scheme for the oxidative cleavage of iron protoporphyrin IX.

[⊗] Abstract published in *Advance ACS Abstracts,* December 15, 1996.

(1) (a) Department of Biochemistry and Molecular Biology and Protein Engineering Network of Centres of Excellence. (b) Biotechnology Laboratory. (c) Present address: W. Alton Jones Cell Science Center, Inc., 10 Old Barn Road, Lake Placid, NY 12946.

(2) Tenhunen, R.; Marver, H. S.; Schmid, R. *J. Biol. Chem.* **1969**, *244*, 6388−6394.

(3) (a) Yoshida, T.; Ishikawa, K.; Sato, M. *Eur. J. Biochem.* **1991**, *199*, 729−733. (b) Wilks, A.; Ortiz de Montellano, P. R. *J. Biol. Chem.* **1993**, *268*, 22357−22362. (c) Yoshinaga, T.; Sudo, Y.; Sano, S. *Biochem. J.* **1990**, *270*, 659−664.

(4) (a) Warburg, O.; Negelein, E. *Chem. Ber.* **1930**, *63*, 1816. (b) Lemberg, R.; Legge, J. W.; Lockwood, W. H. *Nature* **1938**, *142*, 148−149. (c) Kench, J. E. *Biochem. J.* **1954**, *56*, 669−677. (d) Lemberg, R. *Pure Appl. Chem.* **1956** *6*, 1−23.

(5) (a) Lagarias, J. C. *Biochim. Biophys. Acta* **1982**, *717*, 12−19. (b) Sano, S.; Sano, T.; Morishima, I.; Shiro, Y., Maeda, Y. *Proc. Natl. Acad. Sci. U.S.A.* **1986**, *83*, 531−535. (c) Morishima, I.; Fujii, H.; Shiro, Y. *Inorg. Chem.* **1995**, *34*, 1528−1535.

(6) O'Carra, P.; Colleran, E. *FEBS Lett.* **1969**, *5*, 295−298.

S0002-7863(96)02004-5 CCC: $12.00

attack at the four *meso* positions; from the structure of myoglobin, it is clear that the α-*meso* position is the least sterically hindered and most susceptible to attack.[7]

The action of heme oxygenase differs in three important ways from coupled oxidation. First, catalytic turnover of heme oxygenase requires NADPH-cytochrome P-450 reductase as a source of reducing equivalents. Second, the active site of heme oxygenase appears to bind heme with lower affinity and with greater exposure to solvent than is the case for myoglobin or other heme proteins known to undergo coupled oxidation. Finally, heme oxygenase converts heme directly to biliverdin rather than Fe(III)-biliverdin. Interestingly, expulsion of iron from the linear tetrapyrrole in the reaction catalyzed by heme oxygenase appears to be a function of the reductase because replacement of the reductase with ascorbate results in the production of Fe(III)-biliverdin.[3a] On the basis of this information and recent spectroscopic studies with naturally occurring and recombinant heme oxygenase that indicate that the active site of this enzyme is similar in many regards to the active site of myoglobin,[8] it seems apparent that detailed mechanistic understanding of the coupled oxidation of heme bound to the active site of myoglobin can provide information that is likely to be relevant to the initial stages of the reaction by which oxidation of protoheme IX is catalyzed by heme oxygenase.

Experimental Procedures

Protein Expression and Purification. Expression of a synthetic gene coding for horse heart Mb and preparation of variants by site-directed mutagenesis has been described.[9] The Val67Ala/Val68Ser variant was purified according to procedures described for preparation of the wild-type protein.[10] The resulting protein was reconstituted with fresh protoheme IX (Porphyrin Products, Logan, UT) to remove any sulfMb formed during fermentation.[10] Molar absorption coefficients were determined with the pyridine−hemochromagen method.[11] For the Val67Ala/Val68Ser variant, $\epsilon_{408} = 1.68 \times 10^5\ M^{-1}\ cm^{-1}$ (pH 7.0, 25 °C).

Electronic Absorption Spectroscopy. Electronic spectra were collected with a Cary Model 3E (kinetics and pH titration) or a Cary Model 219 (spectroelectrochemistry) spectrophotometer that were equipped with water-jacketed cell holders connected to thermostated water baths and that were interfaced to microcomputers.

Coupled Oxidation Assays. The coupled oxidation of wild-type horse heart metMb (3 μM) and the Val67Ala/Val68Ser variant (5 μM) with ascorbate (1 mM) were monitored spectrophotometrically. The assays were performed aerobically in sodium phosphate buffer (μ = 0.1 M, pH 7.0) at 37 °C. Spectra were recorded (325−700 nm) over a 7 h period. Alternatively, the assays (3 μM protein, 1 mM ascorbate) were performed while monitoring at a single wavelength (408 nm) for 10 h.

Biliverdin Extraction and HPLC Analysis. For analysis of coupled oxidation reaction products, Mb (10 mg metMb in 10 mL of sodium phosphate buffer (pH 7.0)) was reacted (37 °C) with ascorbate (2 mg) for 2 h.[6] The reaction was stopped by cooling the reaction mixture on ice for 15 min, and the biliverdin product was then extracted as follows. Glacial acetic acid (3 mL) and 5 M hydrochloric acid (8 mL) were added to the cooled mixture. The solution was then placed in a 100 mL separatory funnel and extracted with diethyl ether (2 × 15 mL) (BDH). The ether layer contained any unreacted heme and was discarded. The aqueous layer was extracted with chloroform (1 × 5 mL) to remove the biliverdin product, and the chloroform was removed subsequently by evaporation under a stream of argon gas. For HPLC analysis, a fraction of the product as well as the standards (biliverdin, heme, and bilirubin (Sigma)) was dissolved in a minimum volume of DMSO (BDH).

Heme degradation products were analyzed chromatographically with a Beckman System Gold HPLC equipped with a diode array detector. Samples were loaded onto a C-18 reverse-phase column (Alltech, 4.6 mm × 25 cm, 10 μm). All solvents were HPLC grade. Solvent A consisted of 56 parts 0.1 M ammonium phosphate buffer (Fisher) and 44 parts methanol (Fisher). Prior to mixing, the ammonium phosphate buffer was adjusted to pH 3.5 by the addition of phosphoric acid (BDH). Solvent B was 100% methanol. Solvents were filtered and degassed prior to use. The DMSO solutions of reaction products and standards were diluted into solvent A such that 20 μL could be injected onto the column. For analysis, ∼150 pmol of the reaction product, ∼150 pmol of biliverdin, ∼50 pmol of hemin, and ∼100 pmol of bilirubin standard were applied to the reverse-phase column, and the elution profile was monitored at 405 nm.

Analysis of Coupled Oxidation Products by Electrospray Mass Spectrometry. Samples of the Mb-coupled oxidation reaction mixture were analyzed by mass spectrometry to characterize the heme degradation products. The slow rate of Fe(III)-biliverdin formation precluded such an analysis of wild-type Mb, so only the variant was studied in this fashion. An unbuffered solution (5 mL) containing the variant (5 μM) and ascorbate (1 mM) was shaken slowly at 37 °C. A sample (200 μL) of this reaction mixture was removed prior to and 4 h after ascorbate addition. The ascorbate concentration used in this reaction (1 mM) interfered with mass analysis, so the sample was diluted 10-fold and concentrated by centrifugal ultrafiltration (Centricon-10; Amicon) such that the final ascorbate concentration was approximately 0.1 mM (protein concentration ∼5 μM). Prior to injection into the mass spectrometer, methanol was added to the sample to a final concentration of 10% (v/v).

Mass analysis was performed with a triple-quadrupole mass spectrometer equipped with a pneumatically assisted electrospray ion source.[12] A voltage difference of 150 V between the sampling orifice and the skimmer was used to induce collisionally activated dissociation of heme from the Mb samples.[13] Mass analysis was accomplished in the first quadrupole (Q_1). Protein samples were infused continuously into the sprayer needle at a flow rate of 1 μL/min.

Fourier Transform Infrared (FTIR) Spectroscopy. FTIR spectra were recorded at 2 cm^{-1} resolution with a Perkin-Elmer System 2000 spectrometer equipped with a liquid nitrogen cooled mercury cadmium telluride detector. Mb samples were exchanged into sodium phosphate buffer (pH 7.0, μ = 0.1) and concentrated to approximately 3 mM by centrifugal ultrafiltration with an Amicon Centricon-10 unit. A few grains of sodium dithionite (solid) were added to a solution of 50 μL protein to reduce the sample, and a stream of CO gas was passed over the solution for 1 min to convert the sample to the carbonyl form. The sample (25 μL) was loaded into a cell with CaF_2 windows and a 0.05 mm Teflon spacer and placed into a water-jacketed cell holder (Specac, Inc.) connected to a thermostated, circulating water bath. Carbonyl Mb spectra were collected between 1900 and 2000 cm^{-1} (25 °C) and corrected for background absorbance by subtracting a metMb spectrum of similar concentration. An average of 500 scans was used for each spectrum.

Electrochemistry. The reduction potential of the variant (sodium phosphate buffer, pH 7.0, μ = 0.1 M, 25 °C) was obtained with an optically transparent thin-layer electrode ([Mb] = 300 μM; optical pathlength ∼0.02 cm).[14] A mixture of 2-hydroxy-1,4-napthaquinone (45 μM) (Sigma #H-0508), recrystallized $[Ru(NH_3)_6]Cl_3$ [15] (45 μM) (Strem), and $[Ru(NH_3)_5Im]Cl_3$ [16] (45 μM) was used to mediate electron transfer between the protein and the gold electrode. The reference electrode was standardized against the quinhydrone couple, and the resulting potentials were converted to the hydrogen scale as described

(7) Brown, S. B. *Biochem. J.* **1976**, *159*, 23−27. (b) Brown, S. B.; Chabot, A. A.; Enderby, E. A.; North, A. C. T. *Nature* **1981**, *289*, 93−95.
(8) Sun, J.; Wilks, A.; Ortiz de Montellano, P. R.; Loehr, T. M. *Biochemistry* **1993**, *32*, 14151−14157.
(9) Guillemette, J. G.; Matsushima-Hibiya, Y.; Atkinson, T.; Smith, M. *Protein Eng.* **1991**, *4*, 585−592.
(10) Lloyd, E.; Mauk, A. G. *FEBS Lett.* **1994**, *340*, 281−286.
(11) de Duve, C. *Acta Chem. Scand.* **1948**, *2*, 264−289.
(12) Collings, B. A.; Douglas, D. J. *J. Am. Chem. Soc.* **1995**, *118*, 4488−4489.
(13) Feng, R.; Konishi, Y. J. *Biochemistry* **1993**, *33*, 9706−9711.
(14) Reid, L. S.; Taniguchi, V. T.; Gray, H. B.; Mauk, A. G. *J. Am. Chem. Soc.* **1982**, *104*, 7516−7519.
(15) Pladziewicz, J. R.; Meyer, T. J.; Broomhead, J. A.; Taube, H. *Inorg. Chem.* **1973**, *12*, 639−643.
(16) Sundberg, R. J.; Bryan, R. F.; Taylor, I. F.; Taube, H. *J. Am. Chem. Soc.* **1974**, *96*, 381−392.

Table 1. Data Collection and Refinement Parameters

I. Data Collection	
space group	$P2_1$
cell dimensions	
a (Å)	43.00
b (Å)	30.34
c (Å)	57.00
β (deg)	97.55
resolution range (Å)	∞−2.0
total no. of reflns obsd	19 324
no. of unique reflns colld	8607
data completeness (%)	
overall	82.2
inner shell (∞−2.5 Å)	88.0
outer shell (2.5−2.0 Å)	75.9
merging *R* factor (%)[a]	9.7
II. Refinement	
no. of reflns used	8224
resolution range (Å)	8.0−2.0
no. of protein atoms	1239
no. of solvent molecules	120
average thermal factors (Å^2)	
protein atoms	19.6
solvent atoms	38.1
final refinement *R* factor (%)[b]	17.9

[a] $R_{merge} = (\sum_{hkl}\sum_{i=1}^{n}|I_{ihkl} - \bar{I}_{hkl}|)/(\sum_{hkl}\sum_{i=1}^{n}I_{ihkl})$. [b] $R_{cryst} = \sum_{hkl}|F_o - F_c|/\sum_{hkl}|F_o|$.

by Dutton.[17] Trace amounts of *Rhus vernicifera* laccase and catalase (Sigma #C100) were added to maintain anaerobic conditions and to avoid possible complications resulting from peroxide formation. The resulting data were analyzed by fitting to the Nernst equation.

Structural Analysis. Crystals of the Val67Ala/Val68Ser variant of horse heart metMb were grown at room temperature using the hanging drop vapor diffusion technique. Each hanging drop contained 20 mg/mL protein, 20 mM Tris-HCl, 1 mM EDTA, and 60% saturated ammonium sulfate and was adjusted to pH 7.8. Droplets were suspended over crystallization wells having the same components except for the absence of protein and the presence of 68% saturated ammonium sulfate. The crystals obtained were of the space group $P2_1$, with cell dimensions of $a = 43.00$ Å, $b = 30.34$ Å, $c = 57.00$ Å, and $\beta = 97.6°$, and had one molecule per asymmetric unit.

Diffraction data were collected with a Rigaku R-Axis IIC imaging plate area detector system. The incident radiation consisted of Cu Kα X-rays generated by a Rigaku RU-300 rotating anode X-ray generator fitted with a graphite monochromator and operated at 59 kV and 90 mA. The oscillation angle used was 1.8°, and each data frame was exposed for 35 min. A total of 70 data frames were collected and processed using the R-AXIS system software.[18] Details related to diffraction data collection and processing are summarized in Table 1.

A molecular replacement approach (XPLOR 3.1[19]) was used to position a preliminary model of the variant Mb within its unit cell. This starting model consisted of the structure of the wild-type protein[20] in which valines 67 and 68 were both truncated to alanines. Following initial rotational and translational placement, the *R* factor for this model was 36.7% using data from 8.0 to 3.0 Å resolution. Further individual atomic positional and thermal factor refinement decreased the *R* factor to 23.2%, with the data included extended to 2.5 Å resolution.

Following this preliminary refinement, $F_o - F_c$ and omit difference electron density maps were calculated in the region around residues 67 and 68. These maps were used to confirm the amino acid substitutions made and allowed for placement of the side chain hydroxyl of Ser68. A further complete set of omit maps in which 10 amino acids were sequentially removed over the entire course of all 153 amino acids in the polypeptide chain were also examined for any structural changes. After manual changes, principally to exposed side chains, further positional and thermal factor refinements were carried out on the modified model. This refinement was followed by a round of simulated annealing refinement[21] employing a slow cooling protocol that started at 4500 K and used structure factor data to 2.0 Å resolution. The *R* factor at this point was 21.9%.

Final structural refinement was carried out using a restrained parameter least-squares approach with the program PROLSQ.[22] This refinement involved additional alternating cycles of refinement and manual adjustments based on electron density maps. As part of this process, an extensive search for bound water molecules was conducted using the ASIR method,[23] with subsequent manual verification of the positions identified. All water molecules were refined as neutral oxygen atoms having full occupancy, and only those refining to thermal factors of less than 70 Å^2 were retained in subsequent refinements. A total of 120 water molecules was identified in this way.

At the end of the refinement, the final crystallographic *R* factor obtained was 17.9%, and a summary of other refinement results is presented in Table 1. Table 2 provides an analysis of the stereochemistry of the refined Val67Ala/Val68Ser variant Mb structure and the restraint weights used. An estimate of 0.21 Å can be made for the overall rms coordinate error of the current structure based on a Luzzati plot.[24]

Table 2. Stereochemistry of the Refined Val67Ala/Val68Ser Variant of Horse Heart Myoglobin

stereochemical parameter	rms deviation from ideal values	restraint weight
distances (Å)		
bond (1−2)	0.017	0.018
bond (1−3)	0.033	0.025
bond (1−4)	0.053	0.050
planar restraints (Å)	0.010	0.014
chiral volumes (Å^3)	0.139	0.100
nonbonded contacts (Å)[a]		
single torsion	0.191	0.160
multiple torsion	0.144	0.160
possible hydrogen bond	0.146	0.160
torsion angles (deg)		
planar (0° or 180°)	1.7	3.0
staggered (±60°, 180°)	20.7	20.0
orthonormal (±90°)	39.6	15.0

[a] The rms deviation from ideality for this class of restraint incorporates a reduction of 0.18 Å from the radius of each atom involved in a contact.

Results

Kinetics. The oxidation of heme to Fe(III)-biliverdin following aerobic addition of ascorbate was monitored spectrophotometrically (325−700 nm) for wild-type metMb and the variant (Figure 2). Addition of excess ascorbate to wild-type Mb results in complex time-dependent changes in the electronic absorption spectrum that involve a slow conversion of metMb to oxygenated Mb (λ_{max} (nm) = 418, 542, 580) with subsequent slow decay to the Mb−biliverdin complex. The kinetics of this reaction can be described as the sum of two single-exponential processes (Figure 2A, inset) with $k_1 = 1.6 \times 10^{-2}$ and $k_2 = 1.7 \times 10^{-3}$ min^{-1}. On the other hand, addition of excess ascorbate to the Val67Ala/Val68Ser variant results in a rapid decrease in the absorbance at the Soret maximum (408 nm) (Figure 2) that can also be analyzed in terms of two exponential processes; in this case, $k_1 = 1.1 \times 10^{-1}$ and $k_2 = 5.3 \times 10^{-3}$ min^{-1} (Figure 2B, inset).

This experiment was repeated with a more concentrated sample of the variant to assess better the spectroscopic changes

(17) Dutton, P. L. *Methods Enzymol.* **1978**, *54*, 411−418.
(18) (a) Higashi, T. *J. Appl. Crystallogr.* **1990**, *23*, 253−257. (b) Sato, M.; Yamamoto, M.; Imada, K.; Katsube, Y.; Tanaka, N.; Higashi, T. *J. Appl. Crystallogr.* **1992**, *25*, 348−357.
(19) Brunger, A. T. X-PLOR: *A system for X-ray Crystallography and NMR*; Yale University Press: New Haven, CT, 1992.
(20) (a) Evans, S. V.; Brayer, G. D. *J. Biol. Chem.* **1988**, *263*, 4263−4268. (b) Evans, S. V.; Brayer, G. D. *J. Mol. Biol.* **1990**, *213*, 885−897.
(21) Brunger, A. T. *Acta Crystallogr.* **1990**, *A46*, 585−593.
(22) Hendrickson, W. A. *Methods Enzymol.* **1985**, *115B*, 252−270.
(23) Tong, H.; Berghuis, A. M.; Chen, J.; Luo, Y.; Guss, J. M.; Freeman, H. C.; Brayer, G. D. *J. Appl. Crystallogr.* **1994**, *27*, 421−426.
(24) Luzzati, V. *Acta Crystallogr.* **1952**, *5*, 802−810.

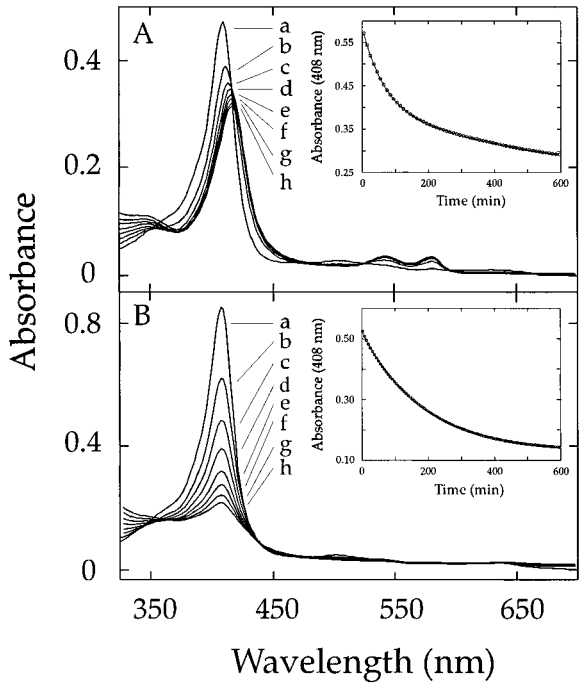

Figure 2. Changes in the electronic absorption spectra (325−700 nm) of wild-type and variant Mbs during coupled oxidation of horse heart Mb (sodium phosphate buffer, $\mu = 0.1$ M, pH 7.0, 37 °C) containing 1.0 mM ascorbate: (A) wild-type Mb (3 μM); (B) Val67Ala/Val68Ser Mb (5 μM). The time after initiation of reaction at which spectra were recorded were as follows: (a) 0 h, (b) 1 h, (c) 2 h, (d) 3 h, (e) 4 h, (f) 5 h, (g) 6 h, (h) 7 h. Inset: change in absorbance monitored at the Soret maximum (408 nm) for (A) wild-type and (B) Val67Ala/Val68Ser Mb during the coupled oxidation reaction with ascorbate; the lines through the data points represent the nonlinear least-squares fits to the data described in the text.

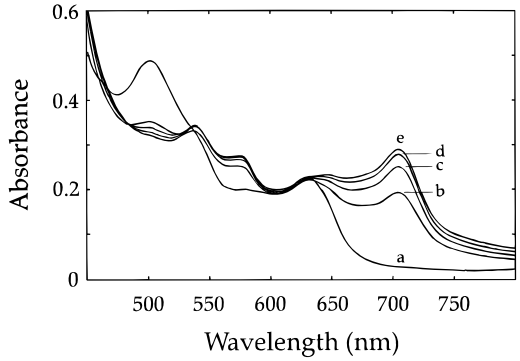

Figure 3. Changes in the electronic absorption spectrum (450−800 nm) of Val67Ala/Val68Ser Mb (50 μM) during coupled oxidation (sodium phosphate buffer, $\mu = 0.1$ M, pH 7.0, 37 °C) in the presence of 10 mM ascorbate.

in the visible region (450−800 nm) (Figure 3). In this experiment, the increase in absorbance at 705 nm that is consistent with Fe(III)-biliverdin formation is notable.[5] The maximum at 705 nm, as well as the broad feature at ∼650 nm that persists throughout the reaction, may also be attributable to one of the intermediates (verdoheme) that is known to form during this reaction.[5] Similar changes are observed in the electronic spectrum of wild-type myoglobin under the same conditions; however, the magnitude of these changes is much smaller, indicating that the amount of verdoheme or Fe(III)-biliverdin formed by this protein is much smaller. Although the Soret region of the variant exhibited no evidence for accumulation of MbO_2 during coupled oxidation (Figure 2) to the extent observed for the wild-type protein, two maxima present in the visible region (539 and 575 nm) may indicate

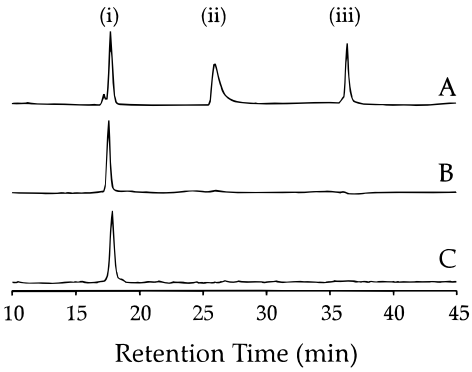

Figure 4. HPLC analysis of product isolated from the coupled oxidation reaction of horse heart Mb with ascorbate: (A) standard mixture of authentic (i) biliverdin, (ii) heme, and (iii) bilirubin; (B) product extracted from wild-type Mb; and (C) the Val67Ala/Val68Ser variant.

the presence of a small amount of oxygenated species (Figure 4). Independent attempts to obtain the electronic spectrum of the oxygenated form of this variant were precluded by rapid autoxidation of the oxyferrous derivative. Alternatively, these visible maxima could result from a small amount of carbonyl-Mb formed during the reaction as a result of CO liberated (Figure 1) by heme degradation.

Analysis of Heme Degradation Products. To assess the identities of the final heme degradation products formed during coupled oxidation of Mb, the reaction mixtures of the wild-type and variant myoglobins were allowed to incubate for 2 h, after which the heme prosthetic groups were then extracted and subjected to analysis by HPLC.[25] Although most of the heme present in the wild-type protein was unreacted under these conditions, sufficient product was formed to permit HPLC analysis. Both the wild-type protein and the variant exhibited a product with a retention time (17 min) that is identical to that exhibited by authentic biliverdin under identical conditions (Figure 4). Conversion of the modified heme products to the corresponding dimethyl ester (DME) followed by HPLC analysis of the DME derivatives demonstrated a single chromatographic component (data not shown) and suggests that the ring opening reaction occurs exclusively at the α-*meso* position[26] as previously observed for the wild-type protein.[6] Notably, this specificity toward oxidation at the α-*meso* carbon is the same as that exhibited by heme oxygenase.[27]

Electrospray mass spectrometry was employed to provide further information concerning the identity of heme degradation products produced during coupled oxidation of the Val67Ala/Val68Ser variant (Figure 5). Analysis of the variant prior to ascorbate addition resulted in observation of the spectrum of unmodified heme ($m/z = 616$) with the expected isotopic distribution (Figure 5A). An identical spectrum was observed for wild-type Mb under these conditions (data not shown). Following addition of ascorbate, similar analysis of the reaction mixture is complicated by a considerable degree of chemical

(25) (a)Bonkovsky, H. L.; Wood, S. G.; Howell, S. K.; Sinclair, P. R.; Lincoln, B.; Healey, J. F.; Sinclair, J. F. *Anal. Biochem.* **1986**, *155*, 56−64. (b) The reaction conditions were scaled-up such that ∼10 mg of wild-type and Val67Ala/Val68Ser Mb were used to ensure enough product for analysis. For wild-type Mb under these conditions, the majority of the heme prosthetic group is unreacted. The conditions and extraction procedures were otherwise the same as those described in the Experimental Procedures.

(26) (a) Four isomeric products are theoretically possible depending on which *meso* carbon is oxidized (α, *β*, *γ*, or *δ*). (b) Products were converted to the DME derivative by the addition of 5% methanolic H_2SO_4 (16 h, 4 °C). The four DME-biliverdin isomers can be separated by HPLC: Noguchi, M.; Yoshida, T.; Kikuchi, G. *J. Biochem.* **1982**, *91*, 1479−1483.

(27) Gray, C. H.; Nicholson, D. C.; Nicolaus, R. A. *Nature* **1958**, *181*, 183−185.

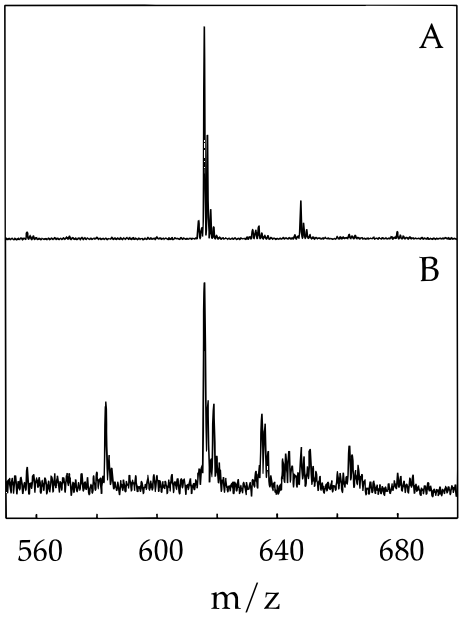

Figure 5. Electrospray mass spectrometry. Only the heme-containing region of the spectrum is shown for the Val67Ala/Val68Ser variant (A) prior to and (B) 4 h after ascorbate addition.

noise resulting from relatively high ascorbate concentration; nevertheless, molecular ions with masses expected for verdoheme (m/z = 619) and Fe(III)-bilverdin (m/z = 635) were observed as coupled oxidation proceeded. Unexpectedly, a molecular ion was also observed that possessed the mass expected for biliverdin (m/z = 583). This positively charged form was also observed when a biliverdin standard was analyzed (data not shown) and may be attributable to a protonated species in solution. The formation of biliverdin may have been facilitated under these conditions because the reaction was performed while shaking in an unbuffered solution.[28]

Spectroscopic Analysis. To elucidate the possible influences of the Val67Ala/Val68Ser substitutions on the manner in which exogenous ligands bind to the heme iron of the variant, the FTIR spectrum of the carbonyl derivative was examined, and the CO stretching frequency, ν_{CO}, was compared with that of the wild-type protein. As previously observed, the predominant ν_{CO} band of wild-type protein occurs at 1945 cm^{-1}.[29] In contrast, the corresponding spectrum of the Val67Ala/Val68Ser variant exhibits two equally intense ν_{CO} bands at 1948 and 1962 cm^{-1} (Figure 6). The ν_{CO} band at 1962 cm^{-1} differs from that observed for other Mb variants with a Ser residue at position 68 and is reminiscent of the spectra of variants possessing a threonyl residue at this position.[30]

Similar to the wild-type protein,[31] the electronic absorption spectrum of the variant is highly pH-dependent (Figure 7). Increasing the pH converts the metaquo form (λ_{max} (nm) = 408, 501, 631) to the hydroxide-bound form (λ_{max} (nm) = 410, 540, 679) with a pK_a for this transition of 9.3. The formation of the hydroxide form of the wild-type protein occurs with a pK_a of 8.9.[31]

Spectroelectrochemistry. A family of spectra collected during a spectroelectrochemical titration of the variant is shown in Figure 8 along with a Nernst plot derived from these data (insert). The spectrum of the reduced form of the variant (λ_{max} (nm) = 432, 558) is similar to that of the wild-type protein.[31] The reduction potential of the variant is −23 mV vs SHE (Nernst slope = 62 mV), which is considerably lower than the corresponding value of 61 mV determined for the wild-type protein under identical conditions (data not shown).

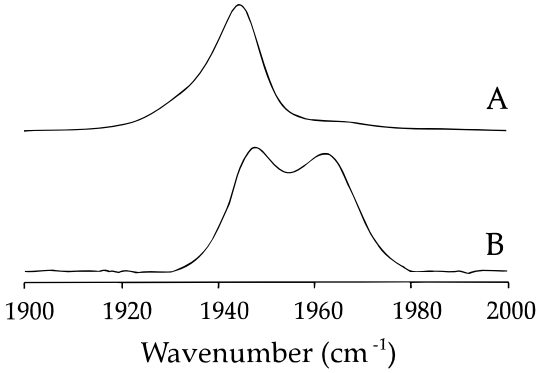

Figure 6. Fourier transform infrared spectra of the carbonyl derivatives of (A) wild-type Mb and (B) the Val67Ala/Val68Ser variant (sodium phosphate buffer, pH 7.0, μ = 0.1, 25 °C).

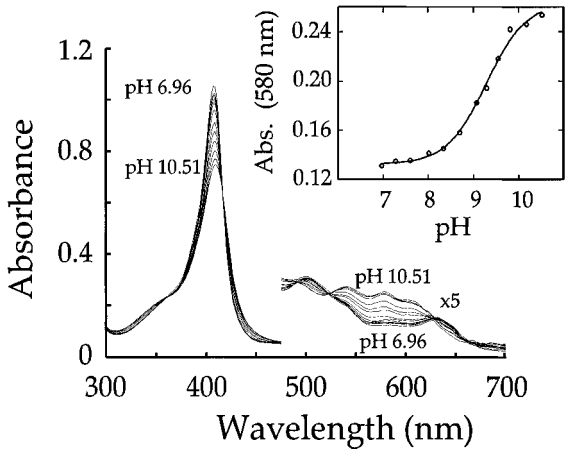

Figure 7. Electronic absorption spectra of Val67Ala/Val68Ser metMb as a function of pH (0.1 M NaCl, 25 °C). The titration was monitored at 580 nm and fit to a single deprotonation process (inset). Above pH 10.5 the variant appears to be unstable.

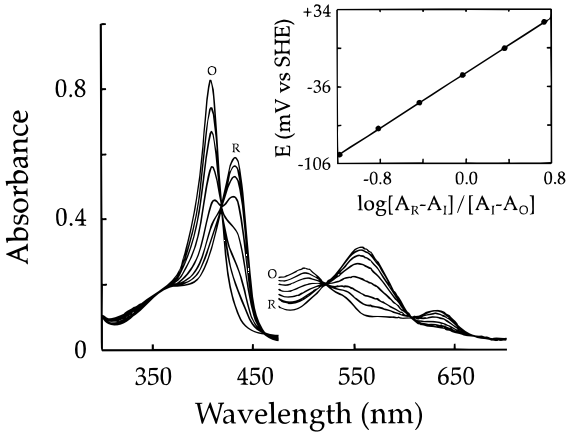

Figure 8. Spectroelectrochemical titration and the corresponding Nernst plot of the Val67Ala/Val68Ser variant (sodium phosphate, pH 7.0, μ = 0.1, 25 °C). Spectra of the completely oxidized (O) and completely reduced (R) species are labeled. The Nernst plot was derived from the dependence of the absorbance at 408 nm on the solution potential.

X-ray Crystallographic Analysis. Structural analysis demonstrates that substitution of an alanine and a serine for Val67

(28) Van Berkel, J. G.; Zhou, F.; Aronson, J. T. *Int. J. Mass Spectrom. Ion Processes*, in press.

(29) Caughey, W. S.; Alben, J. O.; McCoy, S.; Boyer, S. H.; Carache, S.; Hathaway, P. *Biochemistry* **1969**, *8*, 59−62.

(30) An extensive infrared analysis of CO binding to 41 variants of Mb has been reported: Li, T.; Quillin, M. L.; Phillips, G. N.; Olson, J. S. *Biochemistry* **1994**, *33*, 1433−1446.

(31) Antonini, E.; Brunori, M. *Hemoglobin and Myoglobin and Their Reactions with Ligands*; North-Holland: Amsterdam, 1971.

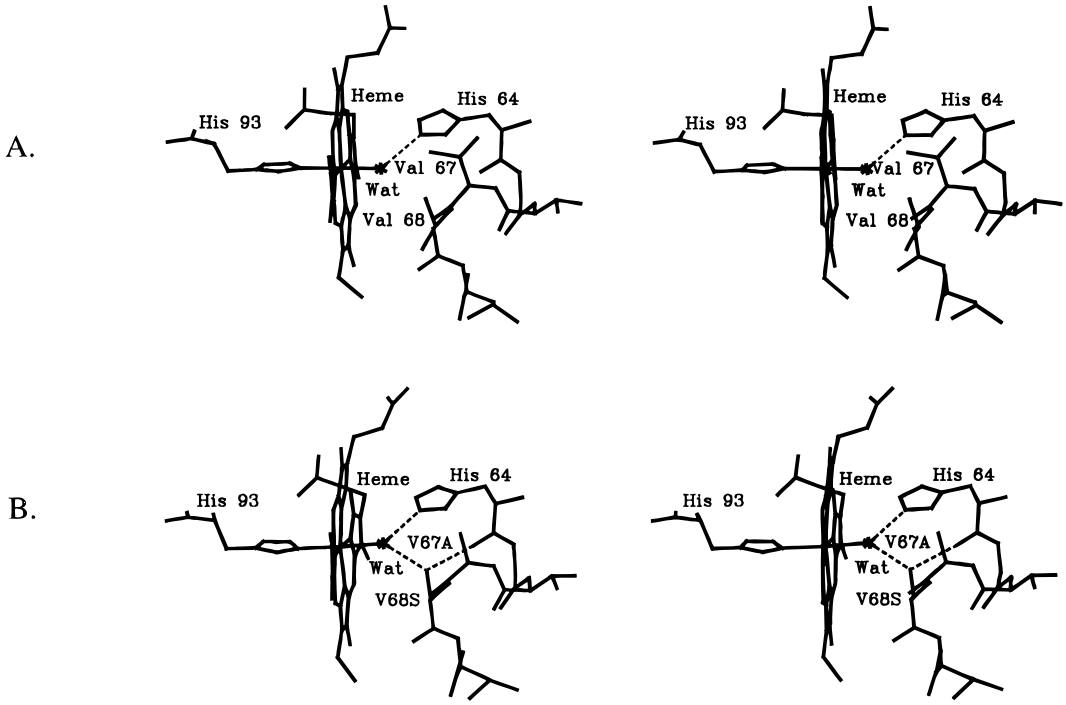

Figure 9. (A) Stereodiagram of the active site of wild-type horse heart myoglobin that indicates the location of Val67 and Val68. (B) Stereodiagram of the active site of the Val67Ala/Val68Ser variant of horse heart myoglobin. Hydrogen bonds are indicated with dashed lines. The presence of Ser68 results in formation of two new hydrogen bonds, one to the water molecule coordinated by the heme iron atom and the other to the carbonyl oxygen atom of His64. Hydrogen bond and ligand coordination distances are provided in Table 3.

Table 3. Hydrogen Bonding and Heme Ligation in the Val67Ala/Val68Ser Variant of Horse Heart Myoglobin

	distance (Å)	
bonded groups	wild-type Mb	Val67Ala/Val68Ser
Fe−His93 NE2	2.20	2.26
Fe−Wat	2.17	2.25
His64 NE2−Wat	2.79	2.52
Ser68 OG−Wat		3.01
Ser68 OG−His64 O		2.78

and Val68, respectively, has minimal impact on the global polypeptide chain fold of horse heart Mb. The largest shifts observed in comparison to the wild-type protein occur at the two termini of the polypeptide chain (residues 1−2 and 148−153) and at the end of an extended surface loop (residues 118−123). These regions are well removed from the site of modification, and their alternative placement likely arises from a combination of positional flexibility, which has been noted earlier in the wild-type protein structure,[20b,32] and new lattice packing interactions formed in the different crystal form of the variant protein.

A detailed comparison of the Val67Ala/Val68Ser variant and wild-type structures in the immediate vicinity of the mutation site is illustrated in Figure 9. The two substituted amino acids retain comparable main chain atom orientations to those of the wild-type protein, as do the β-carbons of their side chains. The Ser68 hydroxyl group has a position corresponding to one of the original wild-type Val68 CG methyl groups. This hydroxyl group forms two new hydrogen bonds, one to the carbonyl group of His64 and the other to the water molecule forming a ligand to the heme iron atom. Table 3 lists the observed hydrogen bond and heme ligand distances in this region.

(32) Maurus, R.; Overall, C. M.; Bogumil, R.; Luo, Y.; Mauk, A. G.; Smith, M.; Brayer, G. D. *Biochim. Biophys. Acta*, submitted.

Discussion

Under the conditions employed in the current study, the coupled oxidation of wild-type Mb can be described as a biphasic process although it is clear that the reaction is more complex than is assumed by such a kinetic analysis (Figure 1). The spectroscopic changes that accompany the coupled oxidation of the wild-type protein provide direct evidence for the formation of oxyMb as the product of the first exponential process. The decay of oxyMb to Fe(III)-biliverdin is also described well as a single-exponential process. HPLC analysis confirms that biliverdin is the final reaction product, but in the case of wild-type Mb, there is no spectroscopic evidence for the presence of any heme degradation intermediates.

The more pronounced and more rapid spectroscopic changes that accompany coupled oxidation kinetics of the Val67Ala/Val68Ser variant can also be described as a biphasic process. It seems unlikely, however, that the rate constants derived from numerical analysis of the kinetics for the wild-type and variant proteins represent the same chemical processes. The accumulation of MbO_2 is less pronounced because the oxygenated derivative of the variant is less stable to autoxidation. The initial kinetically detectable process of this reaction of the variant may arise from the formation of verdoheme, the presence of which was confirmed by electrospray mass spectrometry. Our failure to observe the α-hydroxylheme intermediate by mass spectrometry may simply result from the instability of this species in the presence of oxygen. The second kinetically detectable process probably represents the conversion of verdoheme to Fe(III)-biliverdin. It is possible that the proximity of the serine residue to the oxygen binding site prevents stable interaction between this ligand and ferrous heme and instead directs oxidative attack at the *meso* carbon to produce enhancement of the coupled oxidation reaction of the variant over wild-type Mb.

Although there is no direct evidence for interaction between the serine residue and a bound dioxygen ligand, studies of the

carbonyl derivative may reflect mutation-induced changes at the active site of Mb that are related to the enhanced coupled oxidation observed for the variant. Despite the complex nature of the FTIR spectrum of the variant, the presence of a band at 1962 cm^{-1} is consistent with an increase in the polarity of the active site, such that the $Fe^{\delta(-)}-C\equiv O^{\delta(+)}$ form is partially stabilized by the presence of the electronegative hydroxyl group of Ser68. In terms of active site structure, the increase in polarity could imply that the polar serine residue is positioned close to the iron.

The increase in the pK_a for the heme-bound water ligand as well as the decrease in the midpoint reduction potential suggest that the active site of the variant is more polar than that of the wild-type protein. Definition of the structural basis for the increased polarity of the active site and the effect of the Val68Ser substitution on hydrogen bonding interactions in the distal pocket were sought through determination of the three-dimensional structure of the variant. The structure of this metMb variant confirms that the serine residue at position 68 is within hydrogen bonding distance of the coordinated water molecule. Interaction between this residue and a coordinated dioxygen presumably explains the increased rate of autooxidation exhibited by the variant which, in turn, promotes efficient coupled oxidation of the heme prosthetic group.

Presently, the three-dimensional structure of heme oxygenase has not been determined, so current models of the active site structure of this enzyme are based primarily on spectroscopic studies. This class of enzyme has proved difficult to study in the past because it is membrane-bound, but this problem has been overcome recently by the cloning and expression of a 30 kDa soluble fragment of the enzyme.[3b] Interestingly, the spectroscopic properties of the heme−heme oxygenase complex exhibit greater similarities to those of Mb than to those of peroxidases or cytochrome P-450. At neutral pH, Fe(III)-protoporphyrin IX bound to heme oxygenase is coordinated by an essential histidine and a water ligand with p$K_a \sim 8$.[8,33] The Fe(III)−His stretching frequency of heme oxygenase observed by resonance Raman spectroscopy indicates that the proximal ligand has only a weak (or no) H bond, similar to Mb.[10] A neutral proximal ligand may be an essential determinant of the mechanism of biliverdin formation in heme oxygenase and distinguishes it from the peroxidases and cytochromes P-450 that activate oxygen via heterolytic cleavage of the ligand and ferryl intermediate formation.

Interestingly, the carbonyl derivative of heme oxygenase observed by resonance Raman spectroscopy exhibits a ν_{CO} band at 1958 cm^{-1} [34] that is similar to the band ($\nu_{CO} = 1962$ cm^{-1}) observed in the FTIR spectrum of Val67Ala/Val68Ser Mb. For this reason, it is possible that an electronegative group in the active site of heme oxygenase (e.g., serine or threonine) participates in oxygen transfer from the heme iron to the *meso* position during heme conversion to biliverdin. Recent resonance Raman data suggest that dioxygen coordinates to the heme iron of heme oxygenase in a highly bent, metastable configuration that may facilitate the hydroxylation of the α-*meso* carbon.[35] Finally, the present results indicate that similar studies of other myoglobin variants that exhibit enhanced susceptibility to autoxidation[36] might provide important new insights into the mechanism of coupled oxidation.

Acknowledgment. This work was supported by the Protein Engineering Network of Centres of Excellence, and the FTIR spectrometer was purchased with funds provided by the B.C. Health Care Research Foundation. M.S. is a Career Investigator of the Medical Research Council of Canada. We thank Professor Don Douglas (Department of Chemistry) for access to the electrospray mass spectrometer, Professor Paul Ortiz de Montellano for his comments on the manuscript, and Robert Maurus and Nham Nguyen for helpful discussions and technical assistance.

JA9620043

(33) Sun, J.; Loehr, T. M.; Wilks, A.; Ortiz de Montellano, P. R. *Biochemistry* **1994**, *33*, 13734−13740.

(34) Takahashi, S.; Wang, J.; Rousseau, D. L.; Ishikawa, K.; Yoshida, T.; Takeuchi, N.; Ikeda-Saito, M. *Biochemistry* **1994**, *33*, 5531−5538.

(35) Takahashi, S.; Ishikawa, K.; Takeuchi, N.; Ikeda-Saito, M.; Yoshida, T.; Rousseau, D. L. *J. Am. Chem. Soc.* **1995**, *117*, 6002−6006.

(36) Brantley, R. E.,Jr.; Smerdon, S. J.; Wilkinson, A. J.; Singleton, E. W.; Olson, J. S. *J. Biol. Chem.* **1993**, *268*, 6995−7010.